Semi-global leader-following output consensus of heterogeneous systems with position and rate-limited actuators via state feedback

Panpan Zhou, Ben M. Chen
Department of Mechanical and Automation Engineering, The Chinese University of Hong Kong, Shatin, N.T., Hong Kong
E-mail: ppzhou@mae.cuhk.edu.hk, bmchen@cuhk.edu.hk

Abstract: Inspired by the importance of actuator position and rate constraint, we study in this paper the semi-global leader-following output consensus problem of multiple heterogeneous linear systems in the presence of actuators position and rate saturation via state feedback control. We design a distributed leader state observer, based on which a state feedback output consensus protocol is constructed for each follower. In addition, we propose a framework of formation control by combining consensus control and model predictive control to resolve the problem of obstacle and inter-agent collisions. The effectiveness of our approach is verified by simulation and actual flight experiments of UAVs.

Key Words: Multi-agent systems, Actuator position and rate saturation, Low gain feedback, Collision avoidance.

1 Introduction

Leader-following consensus, a fundamental problem of distributed control for multi-agent systems, entails the construction of a control protocol for every agent so that the states/outputs of all followers converge to the state/output of the leader, see [1–3]. In real applications with substantial number of agents, to reduce communication pressure, distributed control protocols are preferred.

In the early literature, many results are obtained in the consensus problem of a multi-agent system. Li et al. solved the problem of general linear systems with adaptive dynamic protocols [4] and fully distributed control laws [5]. Ma and Miao [6] and Han et al. [7] focused on the output consensus of heterogeneous linear systems via an output regulation approach. It is well noted that actuator saturation is ubiquitous in practical control systems, however, these early results do not take it into consideration.

In view of semi-global convergence with actuator saturation, low gain feedback design technique (see Lin [8]) is of great significance in guaranteeing the control input to remain unsaturated by tuning the low gain parameter small enough, given any arbitrarily large and bounded set of initial conditions. Via the low gain feedback design technique, the semi-global output containment control of multiple linear systems (see [9]) and multiple heterogeneous linear systems (see Shi et al. [10]) are solved. In our recent work [11], a formation control of UAVs are considered by using the semi-global consensus control laws for general linear systems, based on the low gain feedback design technique.

Besides the position saturation of actuators, actuator rate saturation may worsen the performance of the closed-loop system, and may even leads to instability. As reported in [12], actuator saturation is exactly a contributing factor for the mishaps of YF-22 fighter aircraft. The position and rate-limited case is firstly studied by Lin [13] to solve the semi-global stabilization problem of a linear system if the open-loop system is stabilizable and all its poles located at the closed left-half complex plane. In recent years, the methods of Lin [13] is extended to the coordination control of multiple linear systems subject to actuator position and rate saturation. The semi-global containment control and leader-following consensus problems are, respectively, considered by Zhao and Lin [14] and Zhao and Shi [15], where both state feedback control algorithm and output feedback control algorithm are proposed under connected undirected graphs. To the best of our knowledge, there is no results on the output consensus problem for multiple heterogeneous systems with both actuator position and rate saturation, which is exactly the problem we consider in this paper. By the low gain approach and output regulation theory, we construct a state feedback consensus protocol for each follower over a directed network. The protocol is designed based on a distributed observer that estimates the state of the leader. A discrete-time counterpart of this paper can be found in [16].

However, some inherent constraints of the above algorithms prevent them to be effective in real applications. (i) The trajectory of the leader is determined by its initial state. Though the leader has control input in some results [17], the trajectory of the leader is given by a human operator. Hence, the leader cannot generate safe trajectories autonomously to react to environments. (ii) States of agents may exceed the constraint. (iii) They do not take inter-agent collision avoidance into consideration. In this paper, model predictive control (MPC) is applied to tackle these issues.

MPC is actually an optimization problem that can address state and input constraints. It is frequently used in industry for motion planning of a single vehicle. For motion planning of multi-agent systems, inter-vehicle collision avoidance must be taken into consideration, which is a coupled constraint for agents. To solve the coupled constraint in a distributed way, each robot solves a local de-coupled subproblem in a sequential order [18], or applies alternating direction method of multipliers scheme [19] so that computational load is distributed. In this paper, we use the method of Lai et al. [23], that use MPC for motion planning of a single agent, to multi-agent systems.

The contributions of this paper are fourfold: i) for the out-

This paper was supported by in part the Research Grants Council of Hong Kong SAR (Grant No: 14209020), and in part by Peng Cheng Laboratory.

put consensus problem, both actuator position and rate saturation are considered for heterogeneous multi-agent systems; ii) a novel framework of formation control using consensus-based control and MPC is proposed to avoid obstacle collision and inter-agent collision, so that the control law can be implemented in obstacle-cluttered environments; iii) compared with many results where the trajectory of the leader is given by a human operator, the trajectory of the leader in this paper is computed distributed by the agents, via the communication graph; and iv) compared to the work of Lai et al. [23], a novel navigation function is used to avoid local minima, and it leads to a shorter path. Furthermore, actual flight experiments are done to verify our method.

The outline of the rest of this article is as follows. Section 2 gives the problem definition of semi-global state feedback leader-following output consensus for heterogeneous linear systems with position and rate-limited actuators. The consensus protocol is then constructed in Sections 3. In Section 4, we propose a framework of formation control by combining consensus control and MPC to resolve the problem of obstacle and inter-agent collisions. Section 5 gives both the simulation and experiment results. Finally, we conclude our work in Section 6 with some remarks.

Throughout this paper, for a time constant $T \geq 0$ and a signal $x : \mathbb{R}_+ \to \mathbb{R}^s$, $x = [x_1, x_2, \cdots, x_s]^{\mathrm{T}}$, $|x|$ denotes the Euclidean norm, $\|x\|_\infty = \max_i |x_i|$, and $\|x\|_{\infty,T} = \sup_{t\geq T} |x|$.

2 Preliminaries and formulation of the output consensus problem

The group of $(N+1)$ heterogeneous linear systems is consist of one leader and N followers. The leader agent is labeled as 0, and its dynamics is described as

$$\begin{cases} \dot{w} = Sw, \\ y_0 = -Qw, \end{cases} \tag{1}$$

where $w \in \mathbb{R}^s$, $y_0 \in \mathbb{R}^m$ are, respectively, the system state and output. Following the system in [20], the dynamics of the ith follower, $i = 1, 2\cdots, N$, is subject to actuator position and rate saturation:

$$\begin{cases} \dot{x}_i = A_i x_i + B_i \sigma_p(s_i) + W_i w, \\ \dot{s}_i = \sigma_r(u_i), \\ y_i = C_i x_i, \\ e_i = C_i x_i + Qw \quad i = 1, 2, \cdots, N \end{cases} \tag{2}$$

where $x_i \in \mathbb{R}^{n_i}$, $y_i \in \mathbb{R}^m$, $u_i \in \mathbb{R}^{q_i}$ are the plant state, output and control input, respectively, of the ith follower. The second equation represents the actuator dynamics with state $s_i \in \mathbb{R}^{q_i}$. $e_i \in \mathbb{R}^m$ denotes output tracking error of the ith follower. The leader generates both the trajectories to be tracked y_0 and external disturbances to be rejected $W_i w$. $\sigma_p(\cdot) : \mathbb{R}^{q_i} \to \mathbb{R}^{q_i}$ represents a vector valued saturation function. For $s_i = [s_{i1}, s_{i2}, \cdots, s_{iq_i}]^{\mathrm{T}}$, $\sigma_p(s_i) = [\sigma_p(s_{i1}), \sigma_p(s_{i2}), \cdots, \sigma_p(s_{iq_i})]^{\mathrm{T}}$. For each $j = 1, 2, \cdots, q_i$, $\sigma_p(s_{ij}) = \mathrm{sgn}(s_{ij}) \min\{|s_{ij}|, p\}$ is the standard saturation function, where p is a known constant.

The communication topology among the $(N+1)$ agents is represented by a directed graph $\mathcal{G} = \{\mathcal{V}, \mathcal{E}\}$ (see [21] for a summary of digraph). We use $\mathcal{F} = \{1, \cdots, N\}$ to denote the set of followers, and use $\mathcal{N}_i := \{j : (j, i) \in \mathcal{E}\}$ to represent the set of neighbors of node i. We use d to represent the diameter of $\mathcal{G}$, which means the longest among all the shortest paths between each pair of robots. For a directed graph $\mathcal{G}$, the adjacency matrix $\mathcal{A} = [a_{ij}] \in \mathbb{R}^{(N+1)\times(N+1)}$ is defined as $a_{ij} = 1$ if $(j, i) \in \mathcal{E}$, otherwise, $a_{ij} = 0$. The Laplacian matrix $\mathcal{L} = [l_{ij}] \in \mathbb{R}^{(N+1)\times(N+1)}$ is defined as $l_{ij} = -a_{ij}$ if $i \neq j$, and $l_{ii} = \sum_{j=0}^{N} a_{ij}$. According to the classification of the leader and the followers, $\mathcal{L}$ can be partitioned as $\begin{bmatrix} 0 & \mathbf{0} \\ \mathcal{L}_{fl} & \mathcal{L}_{ff} \end{bmatrix}$, where $\mathcal{L}_{fl} \in \mathbb{R}^{N\times 1}$, $\mathcal{L}_{ff} \in \mathbb{R}^{N\times N}$.

Assumption 1: There is a directed path from the leader 0 to each follower.

Assumption 2: The following regulator equations

$$\begin{aligned} &\Pi_i S = A_i \Pi_i + B_i \Gamma_i + W_i \\ &C_i \Pi_i + Q = 0, \qquad i = 1, 2\cdots, N \end{aligned} \tag{3}$$

have a pair of solutions $\Pi_i \in \mathbb{R}^{n_i\times s}$ and $\Gamma_i \in \mathbb{R}^{q_i\times s}$.

Assumption 3: For each $i = 1, 2, \cdots, N$, the pair (A_i, B_i) is stabilizable, and all eigenvalues of A_i have non-positive real parts.

Lemma 1 [8]: Suppose Assumption 3 holds. For each $\epsilon \in (0, 1]$, there exists anx unique positive definite matrix $P_i(\epsilon) \in \mathbb{R}^{n_i\times n_i}$, $i \in \mathcal{F}$ of the following parametric algebraic Riccati equation (ARE):

$$A_i^{\mathrm{T}} P_i(\epsilon) + P_i(\epsilon) A_i - 2P_i(\epsilon) B_i B_i^{\mathrm{T}} P_i(\epsilon) = -\epsilon I_{n_i}. \tag{4}$$

In addition, $\lim_{\epsilon\to 0} P_i(\epsilon) = 0$.

Assumption 4: For $i = 1, 2, \cdots, N$, there exists a time $T \geq 0$ and two positive constants δ_p and δ_r, such that $0 < p - \|\Gamma_i w\|_{\infty,T} \leq \delta_p$ and $0 < r - \|\Gamma_i S w\|_{\infty,T} \leq \delta_r$ for all w with $w(0) \in \mathcal{W}_0$, where $\mathcal{W}_0$ is a priori given bounded set.

Remark 1. *Assumption 4 means that w is bounded for all time $t \geq T$. Since w is determined by Eq. (1), it implies that all eigenvalues of S have non-positive real parts, and those eigenvalues with zero real parts are semi-simple. Besides, Assumption 4 also implies $p > \|\Gamma_i w\|_{\infty,T}$ and $r > \|\Gamma_i S w\|_{\infty,T}$. $\Gamma_i w$ and $\Gamma_i S w$ can be viewed as the generalized actuator position and rate of the leader. If the actuator position or rate of the follower is less than the actuator position or rate of the leader, it is impossible for the followers to catch up the leader when it moves at its maximal pace. Thus, Assumption 4 is reasonable in real applications.*

Due to the communication constraints, some followers may not have access of the information of the leader. Thus, firstly, we construct the following distributed observer for each follower to estimate the state of the leader.

$$\dot{\eta}_i = S\eta_i + \mu\Big(\sum_{j=1}^{N} a_{ij}(\eta_j - \eta_i) + a_{i0}(w - \eta_i)\Big), \quad i \in \mathcal{F} \tag{5}$$

where μ is a positive constant such that $(I_N \otimes S - \mu \mathcal{L}_{ff} \otimes I_s)$ is Hurwitz. Such a μ exists because under Assumption 1, all eigenvalues of $\mathcal{L}_{ff}$ have positive real parts (see [22]).

The state feedback-based semi-global leader-following output consensus problem formed by followers (2) and leader (1) is defined as follows.

Problem 1: Consider a multi-agent system consists of followers (2) and leader (1). Assume that Assumptions

1–4 hold. Let $x = [x_1^{\mathrm{T}}, \cdots, x_N^{\mathrm{T}}]^{\mathrm{T}}$, $s = [s_1^{\mathrm{T}}, \cdots, s_N^{\mathrm{T}}]^{\mathrm{T}}$, $\eta = [\eta_1^{\mathrm{T}}, \cdots, \eta_N^{\mathrm{T}}]^{\mathrm{T}}$, $n = n_1 + n_2 + \cdots + n_N$, and $q = q_1 + q_2 + \cdots + q_N$. For a priori given bounded sets $\mathcal{X}_0 \subset \mathbb{R}^n$, $\mathcal{V}_0 \subset \mathbb{R}^q$, $\mathcal{W}_0 \subset \mathbb{R}^s$ and $\mathcal{Z}_0 \subset \mathbb{R}^{Ns}$, construct a state feedback consensus protocol $u_i = f_i(x_i, s_i, \eta_i)$ for each follower, based on the distributed observer (5), such that for $[x^{\mathrm{T}}(0), s^{\mathrm{T}}(0), w^{\mathrm{T}}(0), \eta^{\mathrm{T}}(0)]^{\mathrm{T}} \in \mathcal{X}_0 \times \mathcal{S}_0 \times \mathcal{W}_0 \times \mathcal{Z}_0$, the leader-following output consensus is achieved, that is, for each $i \in \mathcal{F}$, $\lim_{t\to\infty} e_i = 0$.

3 Output consensus control

In this section, we will propose a state feedback consensus protocol for each follower to solve Problem 1. For notational convenience, we denote $P_i := P_i(\epsilon)$ hereafter to represent the solution of algebraic Riccati equation (4). Consider the following output consensus control law:

$$u_i = -\frac{1}{\epsilon^2}\big(B_i^{\mathrm{T}} P_i (x_i - \Pi_i \eta_i) + (s_i - \Gamma_i \eta_i)\big) + \Gamma_i S \eta_i, \quad (6)$$

where Π_i and Γ_i are a pair solution of the regulator equation (3), and η_i is the state of the observer (5).

Theorem 1: Consider a multi-agent system consists of followers (2) and leader (1). Assume that Assumptions 1–4 hold. The low gain state feedback consensus protocols (6) solve Problem 1.

Proof. Denote the estimation error $\tilde{\eta}_i = \eta_i - w$, whose compact form is $\tilde{\eta} = [\tilde{\eta}_1^{\mathrm{T}},\ \eta_2^{\mathrm{T}}, \cdots, \tilde{\eta}_N^{\mathrm{T}}]^{\mathrm{T}}$. By (5), $\tilde{\eta}$ is determined by the following equation:

$$\dot{\tilde{\eta}} = (I_N \otimes S - \mu \mathcal{L}_{ff} \otimes I_n)\tilde{\eta}.$$

Since $I_N \otimes S - \mu \mathcal{L}_{ff} \otimes I_n$ is Hurwitz, then $\lim_{t\to\infty} \tilde{\eta}_i = 0$.

Let $\tilde{x}_i = x_i - \Pi_i w$, it follows that

$$\begin{aligned}\dot{\tilde{x}}_i &= (A_i x_i + B_i \sigma_p(s_i) + W_i w) - \Pi_i S w \\ &= A_i \tilde{x}_i + B_i \sigma_p(s_i) - B_i \Gamma_i w, \end{aligned} \quad (7)$$

where the last equality holds due to the first equation of Assumption 2.

Let $\tilde{x} = [\tilde{x}_1^{\mathrm{T}}, \cdots, \tilde{x}_N^{\mathrm{T}}]^{\mathrm{T}}$, $s = [s_1^{\mathrm{T}}, \cdots, s_N^{\mathrm{T}}]^{\mathrm{T}}$, $\bar{w} = \mathbf{1}_N \otimes w$, $\tilde{\eta} = [\tilde{\eta}_1^{\mathrm{T}}, \cdots, \tilde{\eta}_N^{\mathrm{T}}]^{\mathrm{T}}$, $X = \mathrm{diag}\{X_1, \cdots, X_N\}$, where $X = A, B, P, \Pi, \Gamma$. Then the compact form of (7) is written as

$$\dot{\tilde{x}} = A\tilde{x} + B\sigma_p(s) - B\Gamma\bar{w}, \quad (8)$$

and s satisfies

$$\dot{s} = \sigma_r\Big(-\frac{1}{\epsilon^2} B^{\mathrm{T}} P (x - \Pi\eta) - \frac{1}{\epsilon^2}(s - \Gamma\eta) + \Gamma(I_N \otimes S)\eta\Big). \quad (9)$$

We define the Lyapunov function candidate

$$V = \tilde{x}^{\mathrm{T}} P \tilde{x} + (B^{\mathrm{T}} P \tilde{x} + s - \Gamma\bar{w})^{\mathrm{T}}(B^{\mathrm{T}} P \tilde{x} + s - \Gamma\bar{w}).$$

Notice that V is positive definite.

By Assumption 4, we have

$$\|\Gamma_i w\|_{\infty,T} < p, \quad \|\Gamma_i S w\|_{\infty,T} < r.$$

Because $\lim_{t\to\infty} \tilde{\eta}_i = 0$, it is reasonable to assume that

$$\begin{aligned}\|B_i^{\mathrm{T}} P_i \Pi_i \tilde{\eta}_i\|_{\infty,T} &\le \epsilon^2 \frac{\delta_r}{6}, \\ \|\Gamma_i \tilde{\eta}_i\|_{\infty,T} &\le \epsilon^2 \frac{\delta_r}{6}, \\ \|\Gamma_i S \tilde{\eta}_i\|_{\infty,T} &\le \frac{\delta_r}{6}, \end{aligned} \quad (10)$$

for all $\epsilon \in (0, 1]$ and all initial conditions of $\tilde{\eta}_i(0)$.

For any $[x^{\mathrm{T}}(0), s^{\mathrm{T}}(0), w^{\mathrm{T}}(0), \eta^{\mathrm{T}}(0)]^{\mathrm{T}} \in \mathcal{X}_0 \times \mathcal{S}_0 \times \mathcal{W}_0 \times \mathcal{Z}_0$, $\tilde{x}(T)$ and $s(T)$ belong to bounded sets $\tilde{\mathcal{X}}_T$ and $\mathcal{S}_T$, respectively, independent of ϵ, since they are determined by linear differentiate equations with bounded inputs. According to Remark 1, $w(t)$ is also bounded. Therefore, there exists a bounded set $\mathcal{W}_T$ such that $w(T) \in \mathcal{W}_T$.

Let $c > 0$ be a constant such that

$$\sup_{\epsilon \in (0,1], [\tilde{x}^{\mathrm{T}}(T), s^{\mathrm{T}}(T), w^{\mathrm{T}}(T)]^{\mathrm{T}} \in \tilde{\mathcal{X}}_T \times \mathcal{S}_T \times \mathcal{W}_T} V \le c.$$

Such a c exists because $\tilde{\mathcal{X}}_T$, $\mathcal{S}_T$ and $\mathcal{W}_T$ are bounded, and $\lim_{\epsilon\to 0} P = 0$.

Define $L_V(c) := \{[\tilde{x}^{\mathrm{T}}, s^{\mathrm{T}}, w^{\mathrm{T}}]^{\mathrm{T}} \in \mathbb{R}^{n+q+s} : V \le c\}$. Let $\epsilon^* \in (0, 1]$ be such that, for all $\epsilon \in (0, \epsilon^*]$, $[\tilde{x}^{\mathrm{T}}, s^{\mathrm{T}}, w^{\mathrm{T}}]^{\mathrm{T}} \in L_V(c)$ implies that

$$\begin{aligned}\|B_i^{\mathrm{T}} P_i A_i \tilde{x}_i\|_{\infty,T} &\le \frac{\sigma_r}{6}, \\ \|B_i^{\mathrm{T}} P_i B_i \delta_p(s_i)\|_{\infty,T} &\le \frac{\sigma_r}{6}, \\ \|B_i^{\mathrm{T}} P_i B_i \Gamma_i w\|_{\infty,T} &\le \frac{\sigma_r}{6}. \end{aligned} \quad (11)$$

The existence of such an ϵ^* is due to the fact that $\lim_{\epsilon\to 0} P_i = 0$.

The derivative of V along the trajectories (1), (8) and (9) inside $L_V(c)$ follows

$$\begin{aligned}
&\dot{V} \\
&= \dot{\tilde{x}}^{\mathrm{T}} P \tilde{x} + \tilde{x}^{\mathrm{T}} P \dot{\tilde{x}} + 2(B^{\mathrm{T}} P \tilde{x} + s - \Gamma\bar{w})^{\mathrm{T}}(B^{\mathrm{T}} P \dot{\tilde{x}} + \dot{s} - \Gamma\dot{\bar{w}}) \\
&= \Big(\big(\tilde{x}^{\mathrm{T}} A^{\mathrm{T}} + \sigma_p^{\mathrm{T}}(s) B^{\mathrm{T}} - \bar{w}^{\mathrm{T}} \Gamma^{\mathrm{T}} B^{\mathrm{T}}\big) P \tilde{x} \\
&\quad + \tilde{x}^{\mathrm{T}} P (A\tilde{x} + B\sigma_p(s) - B\Gamma\bar{w})\Big) + 2(B^{\mathrm{T}} P \tilde{x} + s - \Gamma\bar{w})^{\mathrm{T}} \\
&\quad \times \Big(B^{\mathrm{T}} P (A\tilde{x} + B\sigma_p(s) - B\Gamma\bar{w}) + \sigma_r\big[-\frac{1}{\epsilon^2} B^{\mathrm{T}} P (x - \Pi\eta) \\
&\qquad - \frac{1}{\epsilon^2}(s - \Gamma\eta) + \Gamma(I_N \otimes S)\eta\big] - \Gamma(I_N \otimes S)\bar{w}\Big) \\
&= \tilde{x}^{\mathrm{T}}(-\epsilon I_n + 2PBB^{\mathrm{T}}P)\tilde{x} + 2\tilde{x}^{\mathrm{T}} P B \sigma_p(s) - 2\tilde{x}^{\mathrm{T}} P B \Gamma\bar{w} \\
&\quad + 2(B^{\mathrm{T}} P \tilde{x} + s - \Gamma\bar{w})^{\mathrm{T}}\Big(\sigma_r\big[-\frac{1}{\epsilon^2} B^{\mathrm{T}} P \tilde{x} - \frac{1}{\epsilon^2}(s - \Gamma\bar{w}) \\
&\qquad + \Gamma(I_N \otimes S)\bar{w} + \varsigma\big] - \Gamma(I_N \otimes S)\bar{w} + \Theta\Big) \\
&= -\epsilon \tilde{x}^{\mathrm{T}} \tilde{x} + 2\tilde{x}^{\mathrm{T}} P B (B^{\mathrm{T}} P \tilde{x} + \sigma_p(s) - \Gamma\bar{w}) \\
&\quad + 2(B^{\mathrm{T}} P \tilde{x} + s - \Gamma\bar{w})^{\mathrm{T}}\Big(\sigma_r\big[-\frac{1}{\epsilon^2} B^{\mathrm{T}} P \tilde{x} - \frac{1}{\epsilon^2}(s - \Gamma\bar{w}) \\
&\qquad + \Gamma(I_N \otimes S)\bar{w} + \varsigma\big] - \Gamma(I_N \otimes S)\bar{w} + \Theta\Big) \\
&= -\epsilon \tilde{x}^{\mathrm{T}} \tilde{x} + \sum_{i=1}^{N} 2\tilde{x}_i^{\mathrm{T}} P_i B_i (B_i^{\mathrm{T}} P_i \tilde{x}_i + \sigma_p(s_i) - \Gamma_i w) \\
&\quad + \sum_{i=1}^{N} 2(B_i^{\mathrm{T}} P_i \tilde{x}_i + s_i - \Gamma_i w)^{\mathrm{T}}\Big(\sigma_r\big[-\frac{1}{\epsilon^2} B_i^{\mathrm{T}} P_i \tilde{x}_i \\
&\qquad - \frac{1}{\epsilon^2}(s_i - \Gamma_i w) + \Gamma_i S w + \varsigma_i\big] - \Gamma_i S w + \theta_i\Big),
\end{aligned} \quad (12)$$

where

$$\begin{aligned}\varsigma &= \frac{1}{\epsilon^2}B^{\mathrm{T}}P\Pi\tilde{\eta} + \frac{1}{\epsilon^2}\Gamma\tilde{\eta} + \Gamma(I_N \otimes S)\tilde{\eta},\\ \Theta &= B^{\mathrm{T}}P(A\tilde{x} + B\sigma_p(s) - B\Gamma\bar{w}),\\ \varsigma_i &= \frac{1}{\epsilon^2}B_i^{\mathrm{T}}P_i\Pi_i\tilde{\eta}_i + \frac{1}{\epsilon^2}\Gamma_i\tilde{\eta}_i + \Gamma_i S\tilde{\eta}_i,\\ \theta_i &= B_i^{\mathrm{T}}P_i(A_i\tilde{x}_i + B_i\sigma_p(s_i) - B_i\Gamma_i w).\end{aligned}$$

Denote $\phi_i = -B_i^{\mathrm{T}}P_i\tilde{x}_i$, (12) can be rewritten as

$$\begin{aligned}\dot{V} =& -\epsilon\tilde{x}^{\mathrm{T}}\tilde{x} - \sum_{i=1}^{N} 2\phi_i^{\mathrm{T}}(\sigma_p(s_i) - \Gamma_i w - \phi_i)\\ &+ \sum_{i=1}^{N} 2(s_i - \Gamma_i w - \phi_i)^{\mathrm{T}}\Big(- \Gamma_i S w + \theta_i\\ &+ \sigma_r\big[- \frac{1}{\epsilon^2}(s_i - \Gamma_i w - \phi_i) + \Gamma_i S w + \varsigma_i\big]\Big). \quad (13)\end{aligned}$$

According to (10) and (11), we have

$$\begin{aligned}&\|\varsigma_i\| \le \|\frac{1}{\epsilon^2}B_i^{\mathrm{T}}P_i\Pi_i\tilde{\eta}_i\| + \|\frac{1}{\epsilon^2}\Gamma_i\tilde{\eta}_i\| + \|\Gamma_i S\tilde{\eta}_i\| \le \frac{\delta_r}{2},\\ &\|\theta_i\| \le \|B_i^{\mathrm{T}}P_iA_i\tilde{x}_i\| + \|B_i^{\mathrm{T}}P_iB_i\delta_p(s_i)\| + \|B_i^{\mathrm{T}}P_iB_i\Gamma_i w\|\\ &\quad \le \frac{\delta_r}{2}.\end{aligned}$$

(i) First, we consider the case that $\| - \frac{1}{\epsilon^2}(s_i - \Gamma_i w - \phi_i) + \Gamma_i S w + \varsigma_i\| \le r$, that is, $\|s_i - \Gamma_i w - \phi_i\| \le \epsilon^2\frac{\delta_r}{2}$, which implies $\|s_i\| \le \epsilon^2\frac{\delta_r}{2} + \|\Gamma_i w\| + \|\phi_i\|$. Choosing $\epsilon \le \min\Big\{\max\big\{\epsilon : \epsilon \in (0,1], \|\phi_i\| \le \delta_p - \|\Gamma_i w\|\big\}, \sqrt{\frac{2(p-\|\Gamma_i w\|-\|\phi_i\|)}{\delta_r}}\Big\}$. Such an ϵ exists because $\|\Gamma_i w\| < p$ and $\lim_{\epsilon\to 0}\|\phi_i\| = \lim_{\epsilon\to 0}\| - B_i^{\mathrm{T}}P_i\tilde{x}_i\| = 0$. Then, we have $\|s_i\| \le p$, which means $\sigma_p(s_i) = s_i$. It follows that

$$\begin{aligned}&\sigma_r\big[- \frac{1}{\epsilon^2}(s_i - \Gamma_i w - \phi_i) + \Gamma_i S w + \varsigma_i\big] - \Gamma_i S w + \theta_i\\ &\quad = -\frac{1}{\epsilon^2}(s_i - \Gamma_i w - \phi_i) + \varsigma_i + \theta_i, \quad (14)\end{aligned}$$

and

$$2\phi_i^{\mathrm{T}}(\sigma_p(s_i) - \Gamma_i w - \phi_i) = 2\phi_i^{\mathrm{T}}(s_i - \Gamma_i w - \phi_i). \quad (15)$$

Taking (14) and (15) into (13) gives

$$\begin{aligned}\dot{V} =& -\epsilon\tilde{x}^{\mathrm{T}}\tilde{x} - \sum_{i=1}^{N} 2\phi_i^{\mathrm{T}}(s_i - \Gamma_i w - \phi_i)\\ &+ \sum_{i=1}^{N} 2(s_i - \Gamma_i w - \phi_i)^{\mathrm{T}}\\ &\times \big(- \frac{1}{\epsilon^2}(s_i - \Gamma_i w - \phi_i) + \varsigma_i + \theta_i\big)\\ \le& -\epsilon\tilde{x}^{\mathrm{T}}\tilde{x} - 2\sum_{i=1}^{N}\|s_i - \Gamma_i w - \phi_i\|\\ &\times \Big(\frac{1}{\epsilon^2}\|s_i - \Gamma_i w - \phi_i\| - \|\varsigma_i + \theta_i\| + \|\phi_i\|\Big).\end{aligned}$$

There exists an $\epsilon_1^* \in (0,1]$ such that for any $\epsilon \in (0,\epsilon_1^*]$, $\frac{1}{\epsilon^2}\|s_i - \Gamma_i w - \phi_i\| - \|\varsigma_i + \theta_i\| + \|\phi_i\| > 0$, because $\frac{1}{\epsilon^2} \to \infty$ as $\epsilon \to 0$, $\|\phi_i\| \to 0$ as $\epsilon \to 0$, and $\|\varsigma_i + \theta_i\| \le \delta_r$. Thus, we have

$$\dot{V} < 0, \ \ \forall[\tilde{x}^{\mathrm{T}}, s^{\mathrm{T}}, \bar{w}^{\mathrm{T}}]^{\mathrm{T}} \in L_V(c)\backslash\{0\}. \quad (16)$$

(ii) Next, we consider the case that $-\frac{1}{\epsilon^2}(s_i - \Gamma_i w - \phi_i) + \Gamma_i S w + \varsigma_i < -r$, i.e., $s_i - \Gamma_i w - \phi_i > \epsilon^2(r + \Gamma_i S w + \varsigma_i) > 0$.

(a) if $s_i - \Gamma_i w > 0$ and $\phi_i > 0$, then $\sigma_p(s_i) - \Gamma_i w \ge 0$. It follows that (13) can be rewritten as

$$\begin{aligned}\dot{V} \le& -\epsilon\tilde{x}^{\mathrm{T}}\tilde{x} - 2\sum_{i=1}^{N}\|\phi_i\|(s_i - \Gamma_i w - \phi_i)\\ &+ 2\sum_{i=1}^{N}(-r - \Gamma_i S w + \|\theta_i\|)(s_i - \Gamma_i w - \phi_i)\\ =& -\epsilon\tilde{x}^{\mathrm{T}}\tilde{x} - 2\sum_{i=1}^{N}(\|\phi_i\| + r + \Gamma_i S w - \|\theta_i\|)\\ &\times (s_i - \Gamma_i w - \phi_i).\end{aligned}$$

Since $r - \|\Gamma_i S w\| < \delta_r$ and $\|\theta_i\| \le \frac{\delta_r}{2}$, there exists an $\epsilon_2^* \in (0,1]$ such that for any $\epsilon \in (0,\epsilon_2^*]$, $\|\phi_i\| + r + \Gamma_i S w - \|\theta_i\| > 0$. Thus, it follows that Eq. (16) holds.

(b) if $s_i - \Gamma_i w > 0$ and $\phi_i < 0$, then $(s_i - \Gamma_i w - \phi_i)^{\mathrm{T}}(-r - \Gamma_i S w + \theta_i) < 0$ and $-\phi_i^{\mathrm{T}}(\sigma_p(s_i) - \Gamma_i w - \phi_i) > 0$. Then, we have

$$\begin{aligned}\dot{V} =& -\epsilon\tilde{x}^{\mathrm{T}}\tilde{x} - 2\sum_{i=1}^{N}\phi_i^{\mathrm{T}}(\sigma_p(s_i) - \Gamma_i w - \phi_i)\\ &+ 2\sum_{i=1}^{N}(s_i - \Gamma_i w - \phi_i)^{\mathrm{T}}(-r - \Gamma_i S w + \theta_i)\\ \le& -\epsilon\tilde{x}^{\mathrm{T}}\tilde{x} + 2\sum_{i=1}^{N}(-r - \Gamma_i S w + \theta_i + \|\phi_i\|)\\ &\times (s_i - \Gamma_i w - \phi_i) \quad (17)\end{aligned}$$

Similarly, there exists an $\epsilon_3^* \in (0,1]$ such that for any $\epsilon \in (0,\epsilon_3^*]$, $-r - \Gamma_i S w + \theta_i + \|\phi_i\| < 0$. Since $s_i - \Gamma_i w - \phi_i > 0$, we have $\dot{V} \le -\epsilon\tilde{x}^{\mathrm{T}}\tilde{x}$, which means Eq. (16) holds.

(c) if $s_i - \Gamma_i w < 0$ and $\phi_i < 0$, then $s_i < \Gamma_i w < p$. It is easy to verify that Eq. (17) holds.

(iii) Similarly, we can show that (16) holds for the case that $-\frac{1}{\epsilon^2}(s_i - \Gamma_i w - \phi_i) + \Gamma_i S w + \varsigma_i > r$.

In conclusion, we have shown that, for all $\epsilon \in (0,\epsilon^*]$, $\epsilon^* = \min\{\epsilon_1^*, \epsilon_2^*, \epsilon_3^*\}$,

$$\dot{V} < 0, \ \ \forall[\tilde{x}^{\mathrm{T}}, s^{\mathrm{T}}, w^{\mathrm{T}}]^{\mathrm{T}} \in L_V(c)\backslash\{0\}.$$

Hence, we have $\lim_{t\to\infty}\tilde{x}_i = \lim_{t\to\infty}(x_i - \Pi_i w) = 0$ and $\lim_{t\to\infty}(s_i - \Gamma_i w) = 0$, which implies that

$$\lim_{t\to\infty} e_i = \lim_{t\to\infty}(C_i x_i + Q w) = \lim_{t\to\infty}(C_i(\tilde{x}_i + \Pi_i w) + Q w) = 0.$$

The above facts complete the proof. □

4 Formation control with collision avoidance

In this section, we extend the above results to solve a kind of formation control with obstacle collision avoidance and inter-agent collision avoidance. This section introduces four parts: consensus-based formation control, model predictive control, common obstacle-free convex region, and a framework of formation control.

4.1 Consensus-based formation control

Definition of formation. Consider a set of $m \in \mathbb{N}$ predefined template formations. Each template formation $f \in \mathcal{I} = [1, m]$ is given by a reference point c^f, and agents positions relative to the reference point $\{\Delta\mathrm{p}_1^f, \cdots, \Delta\mathrm{p}_n^f\}$. That is, the absolute position of agent i is actually $p_1^f = \mathrm{c}^f + \Delta\mathrm{p}_i^f$. In this paper, we assume template formations have priority. For example, square has higher priority than line.

Suppose that systems (1) and (2) represent a set of robots like unmanned aerial vehicles. More specifically,

$$\begin{cases} \begin{bmatrix} \dot{p}_0 \\ \dot{v}_0 \\ \dot{a}_0 \\ \dot{j}_0 \end{bmatrix} = \begin{bmatrix} 0 & I & 0 & 0 \\ 0 & 0 & I & 0 \\ 0 & 0 & 0 & I \\ 0 & 0 & 0 & 0 \end{bmatrix} \begin{bmatrix} p_0 \\ v_0 \\ a_0 \\ j_0 \end{bmatrix} \\ p_0 = \begin{bmatrix} I & 0 & 0 & 0 \end{bmatrix} \begin{bmatrix} p_0 \\ v_0 \\ a_0 \\ j_0 \end{bmatrix}, \end{cases} \tag{18}$$

$$\begin{cases} \begin{bmatrix} \dot{p}_i \\ \dot{v}_i \end{bmatrix} = \begin{bmatrix} 0 & I \\ 0 & 0 \end{bmatrix} \begin{bmatrix} p_i \\ v_i \end{bmatrix} + \begin{bmatrix} 0 \\ I \end{bmatrix} \sigma_p(a_i) \\ \dot{a}_i = \sigma_r(j_i) \\ p_i = \begin{bmatrix} I & 0 \end{bmatrix} \begin{bmatrix} p_i \\ v_i \end{bmatrix}, \quad i = 1, \cdots, N. \end{cases} \tag{19}$$

where for $i = 0, 1, \cdots, N$, p_i, v_i, a_i and j_i are respectively the position, velocity, acceleration and jerk of the ith robot in the 2-D or 3-D space. It is easy to obtain states w and x_i, outputs y_i, inputs u_i, and matrices S, Q, A_i, B_i, W_i and C_i by comparing systems (1) and (18), (2) and (19). In the formation control, system (18) is assumed to be a virtual leader.

For a template formation f, the formation control is achieved if $\lim_{t\to\infty}(p_i(t) - p_0(t) - \Delta\mathrm{p}_i^f) = 0$. If we remain the state of the virtual leader unchanged, i.e., $x_0 = [p_0^{\mathrm{T}}, v_0^{\mathrm{T}}, a_0^{\mathrm{T}}, j_0^{\mathrm{T}}]^{\mathrm{T}}$, and transform the state and output of the followers into $\hat{x}_i = [(p_i - \Delta\mathrm{p}_i^f)^{\mathrm{T}}, v_i^{\mathrm{T}}]^{\mathrm{T}}$, $\hat{y}_i = p_i - \Delta\mathrm{p}_i^f$, then systems (19) are converted to

$$\begin{cases} \begin{bmatrix} \dot{p}_i \\ \dot{v}_i \end{bmatrix} = \begin{bmatrix} 0 & I \\ 0 & 0 \end{bmatrix} \begin{bmatrix} p_i - \Delta\mathrm{p}_i^f \\ v_i \end{bmatrix} + \begin{bmatrix} 0 \\ I \end{bmatrix} \sigma_p(a_i) \\ \dot{a}_i = \sigma_r(j_i) \\ p_i - \Delta\mathrm{p}_i^f = \begin{bmatrix} I & 0 \end{bmatrix} \begin{bmatrix} p_i - \Delta\mathrm{p}_i^f \\ v_i \end{bmatrix}, \quad i = 1, \cdots, N. \end{cases} \tag{20}$$

It is obvious that the leader-following formation control of systems (18) and (19) is achieved if the leader-following output consensus problem of systems (18) and (20) is solved.

4.2 Model predictive control

Let $u_i(t)$, $x_i(t)$, $t \in [t_0, t_0 + T]$, be respectively the input and system state trajectories of robot i with T being the planning horizon. The local motion planning can be formulated

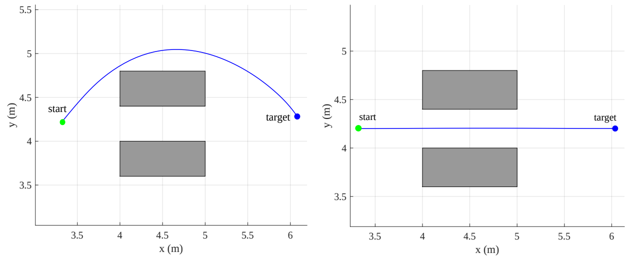

Fig. 1: (left) An example of generated path with local minima without using navigation function; (right) A shorter path is generated by using navigation function. The gray rectangles are obstacles.

as a MPC problem that solves

$$J_i = \xi_i\big(x_i(t_0 + T)\big) + \int_{t=t_0}^{t_0+T} L_i\big(x(t), u(t)\big) \tag{21}$$

$$s.t.\ \ x_i(t_0) = x_{i,0} \tag{22}$$

$$v_i \in [v_{\min}, v_{\max}],\ a_i \in [a_{\min}, a_{\max}],\ j_i \in [j_{\min}, j_{\max}] \tag{23}$$

$$p_i(t) \notin \mathcal{O},\ \ \forall t \geq t_0 \tag{24}$$

$$p_i(t) \cap p_j(t) \in \emptyset,\ \ \forall t \geq t_0, \forall i \neq j \tag{25}$$

where functions ξ_i and L_i are respectively the user-defined terminal and running costs, Eqs. (22)–(25) are respectively the initial condition constraint, state and input constraints, obstacle collision free constraint, and inter-vehicle collision free constraint. $\mathcal{O}$ is a set of static obstacles in the global map. The methods of [23] are summarized as follows:

(a) Given systems (19), the problem is formulated as an optimization problem over continuous-time domain, as Eqs. (21)–(25) shows.
(b) Motion primitives (MPs) are constructed from boundary state constraints, and they are generated offline with a boundary value problem (BVP) solver. These MPs are denoted by boundary state constrained primitives.
(c) Then, the BVP solutions are approximated with a neural network (NN) for fast computation during online trajectory generation.
(d) The references and inputs are generated based on the receding horizon control by solving the MPC problem with NN and particle swarm optimization (PSO).

Its efficiency has been tested on quadrotors in real flight experiments. To apply this algorithm to a multi-robot system, inter-vehicle collision free constraint (25) is considered when solving PSO in step (d). In addition, we use navigation function (NF) as the cost of PSO to improve efficiency of this algorithm.

A navigation function is a special class of artificial potential field that has no local minima. In the left figure of Fig. 1, a path of local minima is generated without using NF. It results in a longer path. NF will address the problem of local minima and generate a shorter path, as the right figure of Fig. 1 shows.

By discretizing the 3-D space, NF is obtained based on Dijkstra's algorithm [24], a commonly used optimal graph search method, by considering Euclidean Distance Transform (EDT) as an additional cost-to-go heuristics. The computation process of NF is given in Algorithm 2. Given a set of targets and the grid map, Algorithm 2 outputs NF of each grid that is stored in a set *dist*. In the grid map *gridMap*, the value of a grid equals one if it is occupied by an obstacle, otherwise, the value is zero. Firstly, NF of each grid is set as infinity (line 2), and each grid is not visited yet (line 3). NF of the target is set as the cost to the nearest obstacle (line 5). When there is at least one grid that has not been visited (line 6), we find the grid *u* that has the minimum NF (line 7), and mark this grid as a visited one (line 8), then we traverse each neighbor of this grid, and the temporary NF of a neighbor *v* equals NF of grid *u* plus the distance of *u* and *v* plus the cost of *v* to its nearest obstacle. If the temporary NF of *v* is less then its previous NF, its NF is updated with the temporary NF (lines 9–15).

Algorithm 1 **Computation of navigation function**

Input: *target*, *gridMap*
Output: *dist* (NF at each grid)
1: **for** each grid *g* in gridMap **do**
2: *dist*[*g*] ← infinity
3: *visited*[*g*] ← 0
4: **end for**
5: *dist*[*target*] ← obsCost(*target*)
6: **while** at least one element of *visited* equals to 0 **do**
7: $u \leftarrow \operatorname{argmin}_u dist[u]$
8: *visited*[*u*] ← 1
9: **for** each adjacent *v* of *u* **do**
10: *preDist* ← *dist*[*v*]
11: *curDist* ← *dist*[*u*] + length(*u*,*v*) + obsCost(*v*)
12: **if** *curDist*<*preDist*
13: *dist*[*v*] ← *curDist*
14: **end if**
15: **end for**
16: **end while**

4.3 Common obstacle-free convex region

Due to limited view of robots, they may have different obstacle maps. Therefore, agents need to reach an agreement of a convex region that is free of obstacles. To this end, we propose a distributed algorithm to obtain the common obstacle free convex region.

To compute $\mathcal{C}_i$, an obstacle-free convex region in field view of robot i, we follow the work of Deits and Tedrake [25], which relies on the iterative optimization. Given a small initial ellipsoid in the obstacle free space of the robot's field of view, we compute i) the separating hyperplanes between obstacles and the ellipsoid; ii) the largest ellipsoid embedded in the convex polytope. The problem is formulated as convex programs and these two steps are repeated until the ellipsoid is convergent. For every obstacle, a hyperplane will be found to separate it and the ellipsoid.

Assume that, for agent i, the separating hyperplanes it obtains are $A_{i,k}x = b_{i,k}$, for $A_{i,k} \in \mathbb{R}^{l_i \times 4}$, $b_{i,k} \in \mathbb{R}^{l_i}$ where l_i is the number of hyperplanes. Then, the convex polytope is the set of points that satisfy

$$\mathcal{C}_i = \{x \in \mathbb{R}^4 | A_i x \leq b_i\}. \tag{26}$$

The intersection of convex polytope of all robots is

$$\mathcal{C} = \cap_{i \in \mathcal{V}} \mathcal{C}_i, \ \forall i, j \in \mathcal{V}, i \neq j. \tag{27}$$

All robots compute the common convex region through an iterative process, as Algorithm 2 shows. For each robot, the separating hyperplanes are initialized as empty sets. Then, the robots communicate to their neighbors only new hyperplanes, to reduce communication cost. At each iteration, the individual convex region shrinks and finally converges to the intersection of convex regions.

Algorithm 2 **Distributed intersection of convex regions**

$A_i(-1) = \emptyset$, $b_i(-1) = \emptyset$, $A_i(0) = A_i(t_0)$, $b_i(0) = b_i(t_0)$
for $k = 0, 1, \cdots, d-1$ **do**
Send $\bar{A}_i(k) = A_i(k) \backslash A_i(k-1)$ and $\bar{b}_i(k) = b_i(k) \backslash b_i(k-1)$ to all $j \in \mathcal{V}_i$
Receive $\bar{A}_j(k)$ and $\bar{b}_j(k)$ from all $j \in \mathcal{V}_i$
$\mathcal{C}_i(k+1) = \text{convhull}(A_i(k), b_i(k), \bar{A}_j(k), \bar{b}_j(k))$
end for

4.4 Framework of formation control using consensus control and MPC

For the trajectory generation of a group of robots, we take receding horizon control (RHC). Each time interval includes two subintervals, which are communication and motion. As Fig. 2 shows, during each cycle, our method consists of the following steps:
(1) At initial time t_0, each robot computes its obstacle-free convex region, denoted by $\mathcal{C}_i$, in position-time space.
(2) All robots compute the common obstacle-free convex region $\mathcal{C}_{ij} = \mathcal{C}_i \cap \mathcal{C}_j$ and $\mathcal{C} = \cap_{i \in \mathcal{V}} \mathcal{C}_i$, $\forall i, j \in \mathcal{V}, i \neq j$.
(3) Each robot uses particle swarm optimization (PSO) to compute the trajectory of the virtual leader;
(4) All robots perform consensus on trajectory of the virtual leader, and the actual trajectory is selected as the one with the minimum cost defined in the PSO algorithm.
(5) All robots reach an agreement on if or not they can keep current formation $f_1 \in \mathcal{I}$ at time $t_0 + \Delta t_3$, within the resulting common obstacle-free convex region $\mathcal{C}$.

(i) If yes, consensus-based formation control is implemented for time $\Delta t_2 - \Delta t_1$. Then, return to Step (1).
(ii) If no, they will try to form other template formations. If one template formation can be formed, for example, formation $f_2 \in \mathcal{I}$, MPC is used for robots to transform from f_1 to f_2. Then, return to Step (1) with the updated formation. If all template formations are failed to form, MPC will be applied for robots to navigate to their goals individually. Then, return to Step (1).

The whole process repeats with updated initial condition until all robots reach their goals.

With consideration of the three issues proposed in Section 1, they are respectively solved by the following methods.
(1) *Trajectory of the leader*. The trajectory of the virtual leader is generated by all the followers. Since dynamics of the virtual leader (18) has zero input, we assume its jerk j_0 keeps a constant during each motion iteration $(t_0, t_0 + \Delta t_2]$. Moreover, the trajectory of the virtual leader is the trajectory of the reference point as described in definition of formation.

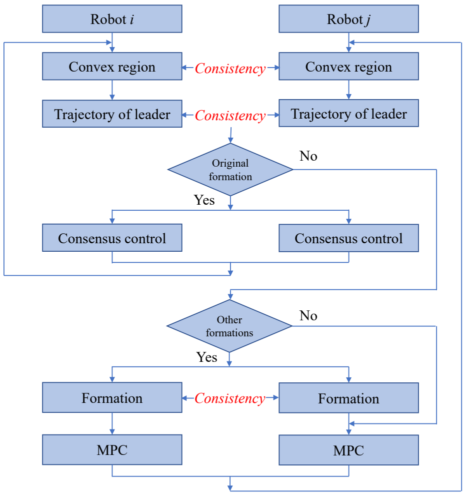

Fig. 2: Overview of the proposed method. The blue parts mean local steps, while the pink parts require robots to communicate to perform parameter consensus.

(2) *State constraint*. Firstly, the state constraint of the virtual leader is satisfied by implementing MPC. Since the consensus control law achieves $\lim_{t\to\infty}(\hat{x}_i - \Pi_i w) = 0$, the state constraint of the followers can be satisfied by setting $x_i(t_0)$ within a small neighborhood of $w(t_0)$. In addition, in such a case, inter-agent collision can also be avoided.
(3) *Collision avoidance*. The inter-agent collision may occur in two conditions. One is the MPC process, which solves the problem as a constraint, as Eq. (25) shows. One is the consensus-based control process. In this case, consensus control is applied only when MPC navigates robots to a small neighborhood of the target formation. Then, robots move in the target formation without inter-agent collision.

5 Simulation and experiment results

In this section, we verify the effectiveness of the framework by both simulations and experiments with a group of micro aerial vehicles whose dynamics satisfy Eqs. (18), (19).

We test our our method in two scenarios. In both scenarios, there are two formation templates: square and line, and square has higher priority than line. The matrix P_i we used in the control law (6) is the solution of Eq. (4) with $\epsilon = 0.1$. Both simulation and experiment are done in a $6\text{m} \times 5\text{m}$ area. The next target is given only if the virtual leader enters the radius (0.2m) of the current one. The algorithm is repeated at 4 Hz, and robots predict formations at 2 Hz. The maximum velocity, acceleration and jerk of robots are 2 m/s, 2 m/s^2 and 1 m/s^3, respectively. For the PSO algorithm, 20 particles are iterated over 20 times.

Scenario 1. The simulation result is shown in Fig. 3. There are four convex obstacles in the area and four targets are given. The initial formation is square. Since square is the predicted formation at each cycle, consensus-based formation control is applied to maintain the square formation.

Scenario 2. The simulation result is shown in Fig. 4. At $t = 2.5$ sec, MAVs can maintain original square formation, so consensus-based control is applied. They arrive at the first target at $t = 5$ sec. At $t = 9.5$ sec, there is a narrow corridor in front of them and they can not pass it if they keep square formation, hence, MPC is used for them to switch to line formation. Afterwards they keep line formation by using consensus-based control until they passed the corridor. At $t = 16.75$ sec, MPC is used to recover to the square formation, given that the square formation is the predicted formation for the next cycle.

The experimental platforms are Crazyflie 2.1, a nano quadrotor helicopter, and we use VICON motion capture system to localize robots and obstacles. The corresponding flight experiments of MAVs in these two scenarios can be found in https://youtu.be/T0JredjnvTs or https://www.bilibili.com/video/BV1qp4y147nG/.

6 Conclusion

In this paper, we have investigated the semi-global output consensus problem for multiple heterogeneous linear systems subject to actuator position and rate saturation. A distributed state feedback-based consensus protocol is constructed for each follower. It is proved that given any a priori given bounded conditions, the problem is solved by the consensus protocol if the communication graph contains a spanning tree. In addition, together with MPC, consensus-based control is applied to solve a kind of formation control with consideration of collision avoidance.

References

[1] S. Dong, W. Ren, and Z. Wu, Observer-based distributed mean-square consensus design for leader-following multiagent markov jump systems, *IEEE Transactions on Cybernetics*, 2019. DOI:10.1109/TCYB.2019.2931196

[2] M. Lu and L. Liu, Leader-following attitude consensus of multiple rigid spacecraft systems under switching networks, *IEEE Transactions on Automatic Control*, 65(2): 839–845, 2019.

[3] Y. Yu, Z. Li, Z. Yang and Z. Ding, Distributed back-stepping consensus protocol for attitude synchronization and tracking on undirected graphs, *Unmanned Systems*, 7(1): 25–32, 2019.

[4] Z. Li, W. Ren, X. Liu and L. Xie, Distributed consensus of linear multi-agent systems with adaptive dynamic protocols, *Automatica*, 49(7): 1986–1995, 2013.

[5] Z. Li, G. Wen, Z. Duan, and W. Ren, Designing fully distributed consensus protocols for linear multi-agent systems with directed graphs, *IEEE Transactions on Automatic Control*, 60(4): 1152–1157, 2014.

[6] Q. Ma and G. Miao, Output consensus for heterogeneous multi-agent systems with linear dynamics, *Applied Mathematics and Computation*, 271: 548–555, 2015.

[7] T. Han, Z. Guan, B. Xiao, J. Wu, and X. Chen, Distributed output consensus of heterogeneous multi-agent systems via an output regulation approach, *Neurocomputing*, 360: 131–137, 2019.

[8] Z. Lin, *Low Gain Feedback*, Springer, 1999.

[9] L. Shi and Z. Lin, Semi-global output containment control of linear multi-agent systems with actuator saturation, in *Proceedings of the 37th Chinese Control Conference*, 2018: 7160–7165.

[10] L. Shi, Y. Li, and Z. Lin, Semi-global leader-following output consensus of heterogeneous multi-agent systems with input saturation, *International Journal of Robust and Nonlinear Control*, 28(16): 4916–4930, 2018.

[11] P. Zhou and B. M. Chen, Semi-global leader-following consensus-based formation flight of unmanned aerial vehicles, *Chinese Journal of Aeronautics*, 2021. DOI:10.1016/j.cja.2021.02.013.

[12] M. Dornhein, Report pinpoints factors leading to YF-22 crash, *Aviation Week & Space Technology*, 9: 53–54, 1992.

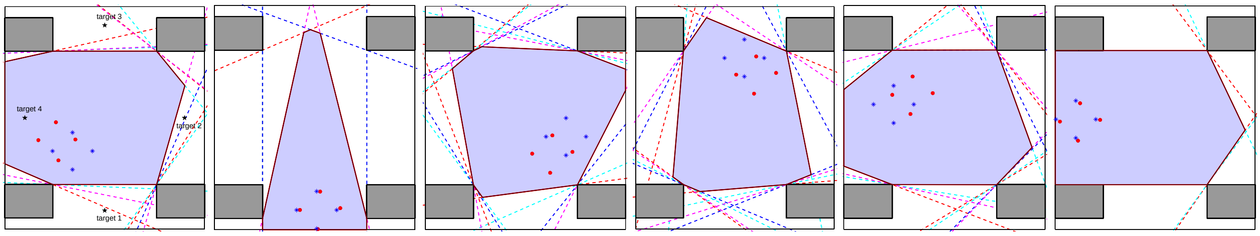

(a)

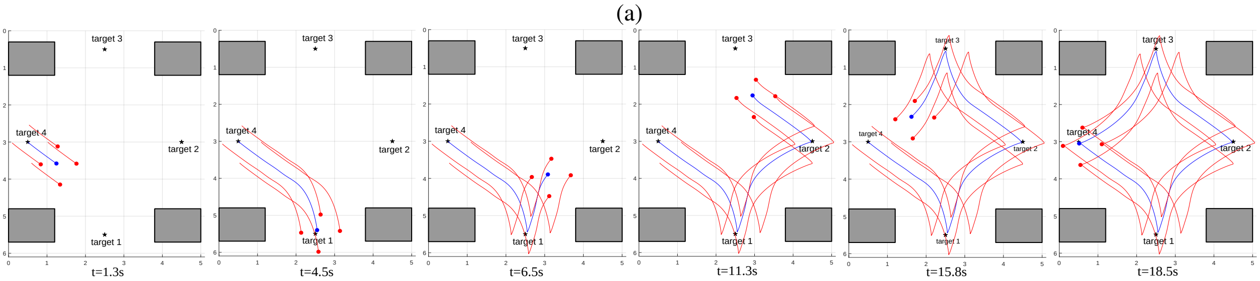

(b)

Fig. 3: Simulation results of Scenario 1. (a) Snapshots of obstacle-free convex regions (light purple area), robot positions (red dots) and target formation (blue stars); (b) Snapshots of trajectories of four MAVs' (red line) and the virtual leader (blue line).

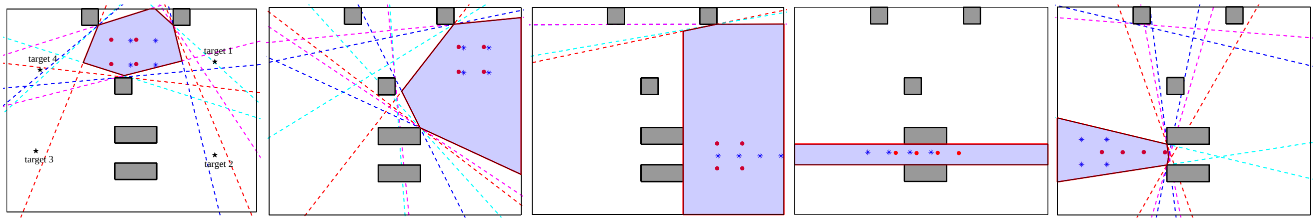

(a)

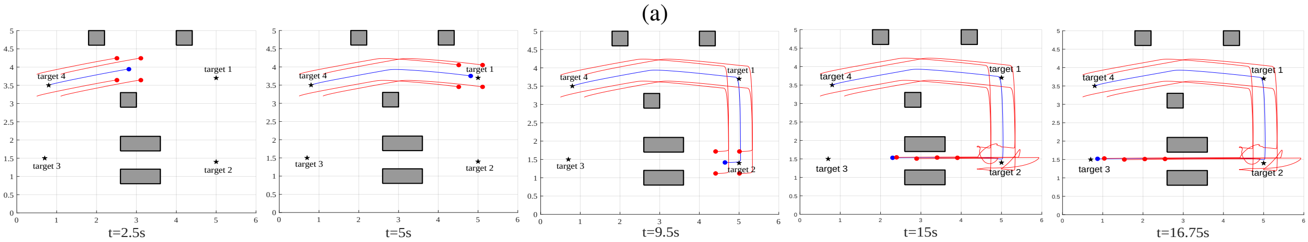

(b)

Fig. 4: Simulation results of Scenario 2.

[13] Z. Lin, Semi-global stabilization of linear systems with position and rate-limited actuators, *Systems & Control Letters*, 30(1): 1–11, 1997.

[14] Z. Zhao and Z. Lin, Semi-global leader-following consensus of multiple linear systems with position and rate limited actuators, *International Journal of Robust and Nonlinear Control*, 25(13): 2083–2100, 2015.

[15] Z. Zhao and H. Shi, Semi-global containment control for linear systems in the presence of actuator position and rate saturation, *International Journal of Robust and Nonlinear Control*, 29(1): 1–18, 2019.

[16] P. Zhou and B. M. Chen, Semi-global leader-following output consensus of discrete-time heterogeneous linear systems with position and rate-limited actuators via state feedback, to be published in the *proceedings of the 40th Chinese Control Conference*, Shanghai, July 2021.

[17] Y. Hua, X. Dong, G. Hu, Q. Li, and Z. Ren, Distributed time-varying output formation tracking for heterogeneous linear multiagent systems with a nonautonomous leader of unknown input, *IEEE Transactions on Automatic Control*, 64(10): 4292–4299, 2019.

[18] H. Zhu and J. Alonso-Mora, Chance-constrained collision avoidance for MAVs in dynamic environments, *IEEE Robotics and Automation Letters*, 4(2): 776–783, 2019.

[19] R. Van Parys and G. Pipeleers, Distributed MPC for multi-vehicle systems moving in formation, *Robotics and Autonomous Systems*, 97: 144–152, 2017.

[20] Z. Lin, M. Pachter, S. Banda, and Y. Shamash, Feedback design for robust tracking of linear systems with rate limited actuators, in *Guidance, Navigation, and Control Conference*, 1997: 3609.

[21] C. Godsil and G. F. Royle, *Algebraic Graph Theory*, Springer, 2013.

[22] Y. Hong, X. Wang, and Z. Jiang, Distributed output regulation of leader–follower multi-agent systems, *International Journal of Robust and Nonlinear Control*, 23(1): 48–66, 2013.

[23] S. Lai, M. Lan, and B. M. Chen, Model predictive local motion planning with boundary state constrained primitives, *IEEE Robotics and Automation Letters*, 4(4): 3577–3584, 2019.

[24] E. W. Dijkstra, A note on two problems in connexion with graphs, *Numerische Mathematik*, 1(1): 269–271, 1959.

[25] R. Deits and R. Tedrake, Computing large convex regions of obstacle-free space through semidefinite programming, in *Algorithmic Foundations of Robotics XI*, 2015: 109–124.